Environmental drivers of fire severity in a large forest fire in SE Spain

Viedma O.[1], Moreno, J.M.[1], Chico, F. [2], Fernández, J.J. [2] and Madrigal, C.[2]

[1] Departamento de Ciencias Ambientales, Universidad de Castilla-La Mancha, Avda. Carlos III, 45071 Toledo, Spain;
[2] Gestión Ambiental de Castilla-La Mancha, S.A. (GEACAM), C/ Río Cabriel, 44, 45007 Toledo, Spain.
olga.viedma@uclm.es; josem.moreno@uclm.es; fernando.chico@geacam.com;
juanjofernandez@geacam.com;carlos.madrigal@geacam.com

Keywords: Burn severity, LiDAR, Sentinel 2, prefire vegetation, fire propagation, fire weather, topography, fire history.

Abstract

Fire severity, understood as a measure of biomass consumption, is a function of dynamical interactions between fuel loads and fire propagation conditions (i.e., fire velocity, wind speed and topography, among other). To understand the factors that control fire severity, accurate methods for estimating pre-fire vegetation structure and composition as well as fire propagation conditions are required. Here we analyzed the spatial variability of fire severity in a large fire having different fuel loads (structure and composition), fire propagation conditions and fire history. The study site was a large and mixed severity fire (3.217 ha) occurred in southeast Spain (Yeste, Albacete) from 27th July to 1th August 2017 that reburned part of an old fire occurred in 1994.

Fire severity was estimated using RBR (Relativized Burn Ratio) derived from Sentinel 2A images, which were validated with Composite Burnt Index (CBI) field plots (n=18). Pre-fire vegetation conditions were derived from: 1) LiDAR metrics at 10 and 30 m pixel size and, 2) other auxiliary data derived from Sentinel 2A, the 4th National Forest Inventory (NFI) and National Forest Map (NFM). Fire propagation conditions for different burning periods were estimated based on a fire progression map. In addition, weather conditions for each burning period were obtained from a nearby automated weather station. Moreover, directional (i.e., in the sense of the propagating front along the fire perimeter) slope and wind speed were calculated for each burning period. Regression models between fire severity and its driving factors were obtained applying Boosted Regression Trees (BRTs).

Fire severity was best explained by burning conditions (cross-validation correlation [CVC] 0.70), followed by prefire stand structure derived from Lidar at 30 m and other auxiliary variables (CVC 0.48 for both models). Combining those sets of variables, CVC increased to 0.80. Yet, the variables that most contributed to the model was fire rate of spread (14.6%) and LAI (12.5%). Higher fire severity occurred in elevated areas, burning uphill, with high fire rate of spread, with dominant winds (mainly from the West) blowing windwards of the fire-front and under extreme weather conditions. Moreover, fire severity was high in shrublands and Pinus forests (*P. pinaster* and *P.halepensis*) with small trees and abundant understory. Based on the dominant winds and topography fuel management practices could be carried out in a way to limit fire severity, thus allowing a better control of fire.

Methodology

1) The study area

The study area was the Yeste fire (Albacete province, SE Spain), that occurred in 2017 (Fig. 1).The fire started on July 27th and was controlled on August 1st, after burning 3.217 ha. This was a topographical fire with wind phases that spread with high intensity as a surface fire and as a passive crown fire with emission of secondary focuses. Fire weather conditions were characterized by dominant winds from the W-NW direction that alternated with E direction. The temperature was maintained with maxima around 38-40 ºC and minima that did not fall below 20 ºC. Relative

humidity peak was 25%, with very lowest values of < 5 %. The burned area was mainly covered by dense Pinus forests (i.e., *Pinus pinaster*, *Pinus halepensis* and in a lesser extent *Pinus nigra*) (44%), scattered Pinus forests with high understory (40%) and shrublands (*Juniperus oxycedrus* and *Arbutus unedo*) (16%).

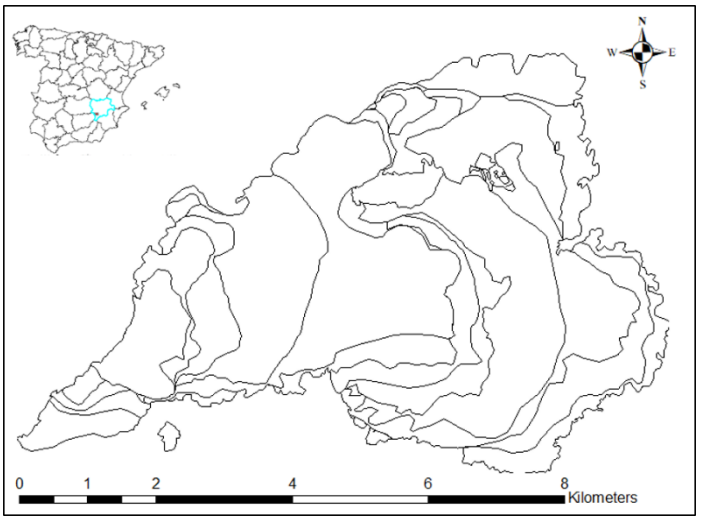

Figure 1. Localization map of Yeste fire (Albacete, Spain) and map of the fire advance (isochrones).

2) Prefire vegetation

a. Lidar processing and derived products

i. Lidar processing from LasTools

Lidar pre-processing was carried out using LasTools software (Isenburg 2014). Lidar data quality was checked generating textual reports (*lasinfo*), making sure alignment and overlap between flightlines (*lasoverlap*), and measuring pulse density per square meter (*lasgrid*). Additional checks for points replication (*lasduplicate*) was also performed. From *lasinfo* we assessed that there were up to 4 returns per pulse; the average point density (per square meter) was 1.29 for all returns and 1.11 for last returns only, and that the average point spacing was 0.88 meters for all returns, 0.95 for last returns only. For rasters of 2 x2 m cell size, the average point density was 2 * 2 * 1.11 = 4.4 points per cell. To facilitate laser point processing (24 large files covering an area 95.37 km^2) we divided the dataset into manageable tiles (polygons) of < 500 MB using *lastile* and a buffer of 50 meters around every tile. This buffer helped to reduce edge artifacts at the tile boundaries. Then, LiDAR points were filtered for noise using *lasnoise*, andadditional denoise filter (Statistical Outlier Removal filter [SOR] with default settings) from CloudCompare software (http://www.cloudcompare.org/) reducing considerably the proportion of noise points. Finally, to speed up most following processing steps, we used *lassort* to rearrange laser points into a space-filling curve order, and *lasindex* to give spatial indexing information to the tiles.

After pre-processing Lidar files, ground returns were classified using the Progressive Triangulated Irregular Network (i.e. a Delaunay TIN) densification algorithm implemented in *lasground*. This tool implements the method proposed by Axelsson (2000), which is based on a grid simplification. The pulse density of 1.1 shots per square meter supported a resolution of 1 meter for the raster DTM. *Lasground* was run on last returns leaving out noise and overlapped points (classes 7 and 12, respectively). The parameterization of *lasground* consisted of the selection of two settings: i) the terrain type, that was modulated by step sizes varying from 3 to 25 (3 [*-wilderness*],5 [*-nature*],10 [*-town*] and 25[*-default*]) and, ii) the granularity, i.e., how much computational effort to invest into finding the initial ground estimate using the switches '*-extra_fine*' and '*-hyper_fine*'. Moreover, we fine-tuned the algorithm by specifying :

1) different threshold in meters at which *spikes* are removed from the ground: 0.5, 1 and 3 m, and 2) the maximal *offset* in meters up to which points above the current ground estimate are included: 0.05, 0.2 and 0.4 m. Later, we made a sensitiviy analysis of those settings for the accuracy of the derived products.

Using large step sizes or small spike and offset values (e.g.-town [-step 10m] or –wilderness [spike 1 and offset 0.05]), there were several ground modeling errors in steep slopes, cliffs and deeply incised stream banks that were classified as non-ground (Type I error); but there was a good classification of understory or low/dense shrubs as non-ground. However, using small step sizes (e.g. –wilderness [-step 3m] with large spike and offset values [spike 3 and offset 0.2], the point classification erroneously included low and dense vegetation as ground (Type II error), but drew perfectly cliffs and steep slopes. Accordingly, we calculated 2 DTMs: one smoother using –town and low spike and offset values (called '*town*' from now on) and other rougher using –wilderness and high spike and offset values ('*wild*'). Finally, we normalized the height of the points above the ground using '*lasheight*', dropping all points that were 30 meters above or 2 m below the ground.

ii. Lidar derived products

The Digital Terrain Model (DTM): we computed the DTM at 1m pixel size from the ground-classified tiles using *las2dem*. The vertical accuracy of the LiDAR data was assessed comparing several profiles collected on asphalt points with the elevations of the national MDT at 5 m pixel size downloaded from the Spanish Geographic Institute (SGI) (www.ign.es).

A spike-free Canopy Height Model (CHM): we used the "spike-free" algorithm (Khosravipour et. al. 2016) to build the CHM at 2 m pixel size. This method resolves the problem of the empty pixels and so called "pits" by the interpolation of first returns with a triangulated irregular network (TIN) (i.e., Contrained Delaunay algorithm) and then, rasterizing it onto a grid. This algorithm is implemented with '*grid_tincanopy*' function in *LidR* package (Roussel and Auty 2018) in R software (R Core Team 2012). Finally, we calculated two CHMs using the two DTMs created (i.e., *town* and *wild* models). The deficiencies found on both of them were corrected by a masking approach (not shown here), creating a '*composed*' CHM.

Tree detection and crown segmentation: Tree top detection was based on local maxima filter applied on gridded objects using a moving window of 3x3 m and 4 m as minimum tree height by using '*treetops*' function in *LidR* package. Crown segmentation was achieved with '*lastrees´* function, based on local maxima + Voronoi tesselation using a threshold of 4 meters and default parameters as they are described in Silva et al. (2016). Later, we computed crown metrics with '*tree_metrics*' function: crown area and maximum height (mean, median, sd, min and max) and delineated crown contourns using *raster* package (Hijmans and van Etten 2012) in R software (R Core Team 2012).

Vegetation strata metrics: We used *lascanopy* function in LasTools software (Isenburg 2014) for computing height metrics for the entire area at 10 and 30 m pixel size. For normalized '*Town*' ground points, height metrics were computed using cutoffs ≤ 2 m. For normalized '*Wild*'ground points, we used cutoffs > 2 m. Accordingly, we calculated height metrics for strata between 0.3-1 m and 1-2 m using normalized '*Town*' ground points, and calculated point density for the following height ranges: 0.3-0.6 m, 0.6-1 m and 1-2 m. For normalized '*Wild*' ground points, we calculated height metrics for strata between 2-4 m and > 4 m as well as the point density for several height ranges (from 2 m to 30 m at different steps). Point density was obtained by diving the points at each height range by the total number of points, and scaled to a percentage.

Fuel models map: We obtained fuel models using the Lidar height metrics derived at 30 m and the compositional metrics (i.e., percentage of occupation of different height ranges [(< 0.6 m, 0.6-1 m, 1-2 m, 2-4 m and > 4 m] at 30m pixel size) derived from the '*composed*' CHM. We used the Prometheus classification framework, adding other fuel models types that gathered the variability of vegetation structures found in the study area (i.e., open forests [< 30% trees] and medium dense forest [>30 and < 50% trees]). Vertical continuity was measured as the difference between

minimum height in stratum > 4 m and the maximum height in stratum 2-4 m. If the difference was > 0.5 m there was not vertical continuity otherwise there was continuity.

b. Other vegetation data

i. Vegetation composition and aboveground biomass

Prefire vegetation composition (i.e., dominant and codominant species) was derived from National Forest Map (NFM) at 1:50.000 scale (https://www.miteco.gob.es). Prefire biomass (log transformed) derived from 4th National Forest Inventory (NFI) (http://visores.castillalamancha.es/ginfor/#/app) was estimated for the entire area from Lidar metrics at 10 m (standardized by z-score) and NBR derived from Sentinel 2A using 22 field plots sampled in 3rd and 4th NFIs (with different radii: 15 and 25 m). Predictive models were built using GAMs and linear models (not shown here). Moreover, tree spacing and tree volume was derived from 4th NFI. Finally, the Normalized Burnt Ratio (NBR) and LAI were obtained from the prefire Sentinel 2A image (July 18th 2017).

3) Burning conditions and directional topography

A fire progression map was facilitated by the Forestry Services of Castilla-La Mancha. Based on this, the burned area was divided into 18 burning periods, each corresponding to the area burned during the various times for which we had information about the position of the fire-front (Fig. 1). The burning periods were not of equal duration. They ranged between 1h 30 min and 10h. We calculated two fire propagation-related variables: propagation direction (degrees) and fire rate of spread (m min^{-1}). We used the maximum distance between any two points across the starting and ending fire perimeters of two consecutive burning periods to determine the compass direction and speed of maximum spread of the propagation front (see Viedma et al. 2015 for further details). In addition, the weather conditions for each burning period were calculated using hourly data from an automated weather station located next to the fire. These included mean, minimum and maximum air temperature (ºC), mean air relative humidity (%) wind direction (degrees) and speed (km/h), dew point and potential evapotranspiration (Table 1). Mean and maximum weather variables were assigned to every burning period. Finally, hourly wind direction and wind speed data were spatially-explicit derived at pixel scale (50 m to avoid spurious results) using the wind simulation program WindNinja (Forthofer 2007) in order to obtain the local wind changes caused by topographic variation. Using spatially explicit wind variables and fire propagation directional data, a measure of directional wind speed was derived (see Viedma et al. 2015 for further details). Positive and high values were related to the speed of windwards winds (in the same or close to the fire propagation direction) and low and negative values to slower leeward winds. Finally, a map with the extent of the last fire occurred in 1994 was available.

We used a 5 m resolution DTM from the SGI (www.ign.es) to derive directional slope (degrees) (i.e., the slope as would be seen by the fire as it propagated). Taking into account the changing propagation direction of the fire-front around the fire perimeter, we calculated the directional slope for each of the cells of the burned area at the different periods. Negative values are given for aspects directly opposite to the propagating direction of the fire-front (i.e., upslope-uphill), and positive values for downslope propagation (Table 1). We used SEXTANTE software (www.sextante.com) to calculate it.

4) Statistical analysis

We determined the relationships between RBR-fire severity and the two sets of explanatory variables (prefire vegetation and burning conditions) separating prefire vegetation variables in 3 different subsets: prefire vegetation derived from Lidar metrics at 10m, at 30m and prefire vegetation derived from auxiliary data (NFM, 4th NFI and Sentinel 2A), using Boosted Regression Tree (BRT) models (Elith et al. 2008). First, models were constructed for each sets of variables separately and, later, for the entire set of variables. The BRT approach is a nonparametric machine-learning technique that uses the technique of boosting to adaptively combine large numbers of relatively

simple Regression Tree (RT) models to optimize predictive performance (Elith et al. 2008). The BRT calibration was done following Viedma et al. (2015). BRT models were fitted using a Gaussian data distribution of the response variable (RBR) by applying the *gbm* (Generalized Boosted Regression Models) package (Ridgeway 2007) and code provided by Elith et al. (2008) in R software (R Development Core Team 2012). The predictive performance of all BRT models was assessed on the training data (n= 3497) plus the subset of data that were withheld during cross-validation. For final BRT model, we asessed model performance using external test data (n=1499). Performance measures were: i) percentage of deviance explained (mean residual deviance) from the null deviance (total deviance) using training and cross-validated data, and ii) correlation of the models' fitted values (R), for training and cross-validated data and also, for test data in the case of the final model.

Results

RBR varied between -0.11 and 0.71 in the burned area. Following standard classifications of RBR (Parks et al. 2014), low severity values (< 0.1) comprised 5.2% of the burned area, moderate severity values (0.1- 0.3) 35.2%, and high severity values (> 0.3) 59.5%. The ground-based composite burn index (CBI) was acceptably correlated with RBR (Adjusted R^2=0.64) (see De Santis and Chuvieco [2007] for further details).

Prefire vegetation BRT models (i.e., derived from Lidar metrics at 10m and 30m and other auxiliary data) showed very different ability to explain RBR-fire severity. The most explicative BRT model was that derived from Lidar metrics at 30m, which explained 71% of the total deviance using training data and 25% of the deviance after cross-validation. The correlation coefficient (R) was 0.90 in training and 0.49 after cross-validation correlation (CVC). Density of points in low (until 2 m) and medium (6-8 m) strata as well as intensity values in low (< 2 m) and high (> 2 m) strata were identified as the most important variables (i.e., relative importance in BRTs > 5%). Partial dependence plots of these variables indicated that higher fire severity was related to stands with medium density of trees (< 50%) between 6-8 m of height, with high dispersion in their intensity values (e.g., due to high biomass variability), and also with important understory vegetation < 2 m (with low and homogeneous intensity values). BRTs based on Lidar metrics at 10 m showed an R of 0.52 and a CVC of 0.34; with the most important variables being similar to those selected by the BRT derived from Lidar metrics at 30m (not shown). BRT derived from other vegetation data (NFM, 4th NFI and biophysical variables derived from Sentinel 2A) explained 33% of the total deviance using training data and 25% of the deviance after cross-validation with an R of 0.58 and a CVC of 0.48. LAI derived from Sentinel 2A, vegetation composition, tree volume and tree spacing were the most significant variables. The partial dependence plots indicated that higher fire severity values were found in areas with medium-high LAI values (around 1.5), with low tree volume, and high tree spacing. The species combination more affected by fire were: shrublands with trees (*Juniperus oxycedrus* plus *Pinus halepensis*) followed by Pinus forests of *Pinus pinaster* and *Pinus halepensis*, and shrublands without trees.

The BRT model based on burning conditions and directional topography explained 83% of the total deviance using training data and 50% of the deviance after cross-validation showing a correlation coefficient (R) of 0.93 and a CVC of 0.70. Fire rate of spread, elevation, directional wind speed and wind direction, directional slopes and relative humidity contributed with > 5% to the model. The partial dependence plots indicated that higher fire severity values were found in areas where fire rate of spread was high and fire spread upslope (high and negative directional slopes), winds blew windwards to the fire-front (high and positive directional winds), elevation was low, and weather conditions were extreme (very low air humidity [< 10%] and high mean air temperature [> 34ºC]).

When all the relevant variables were used together, BRT model explained 92% of the total deviance using training data and 67% of the deviance after cross-validation ; the correlation coefficient (R) was 0.97 and CVC was 0.80. For test data (n=1499), the model showed an adjusted R^2 of 0.63. The relevant variables of the combined BRT model included five prefire stand structure variables (LAI, density of points between 1-2 m, dominant and codominant species, intensity dispersion of points at < 2 m and maximum height of stratum > 2 m), directional topography and elevation, and several burning conditions variables (fire rate of spread, directional wind speed and wind direction,

humidity and mean temperature). The partial dependence plots (Fig. 2) showed that fire severity increased greatly when fire rate of spread was high (c.a. 7m/min which was above the 3rd quartile) and fire spread uphill (high negative directional slopes), dominant winds (mainly from the West) blew windwards to the fire-front (high and positive values of directional wind speed variable), mean temperature was high (> 34 ºC) and air humidity was very low (< 10%). Also, fire severity was high over elevated areas (> 1200 m), changing its behaviour when combined with prefire vegetation. In addition, fire severity increased with LAI values above the mean (1.21) and decreased at high LAI values (> 2). The species more negatively affected by fire were shrublands with trees (*Juniperus oxycedrus* plus *Pinus halepensis)* and shrublands, both with LAI values below the mean and with homogeneous and low intensity values, followed by pinus stands (*Pinus halepensis* and *Pinus pinaster*, and viceversa), with LAI values below the 3rd quartile (1.6) and low height (< 5 m). On relative terms, prefire stand structure contributed 48.2% to the model (sum of the relative importance of those variables) and topography and burning conditions (51.8%). Yet, the variables that most contributed to the model was fire rate of spread (14.6%) and LAI (12.5%).

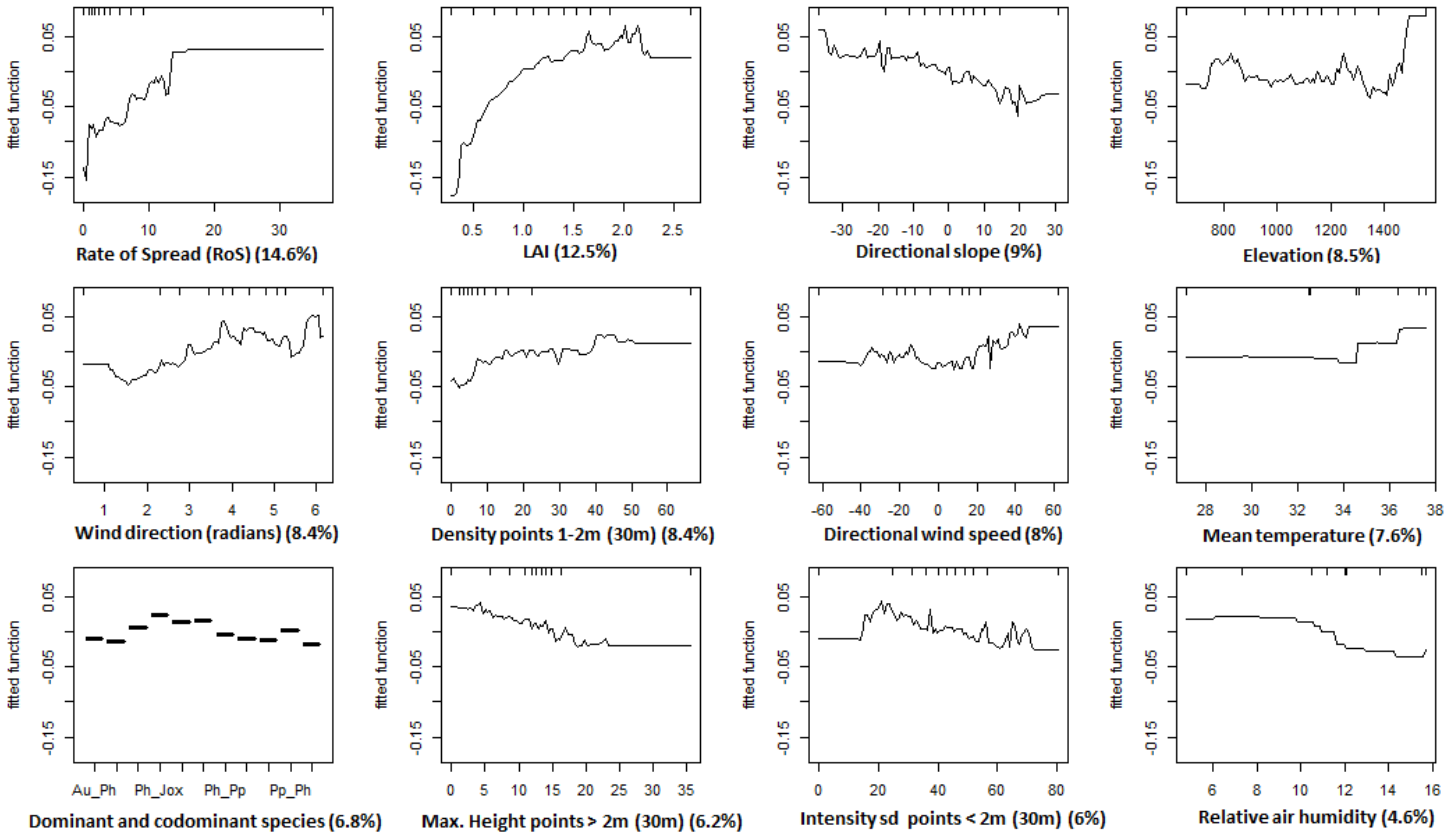

Figure 2. Partial dependence of fire severity (RBR) from the final BRT model based on the entire set of variables (i.e., prefire vegetation burning conditions and directional topography). The y-axis represents the z-score of the RBR and the x-axis the original explanatory variables. In parentheses is showed the relative contribution of each variable.

There were strong interactions among predictions. The relationships between LAI and fire severity was dependent on burning conditions and tree height. Hence, for burned stands with medium-high LAI values, fire severity was higher in those ones affected by high speed windwards winds and those located at elevated areas, with negative directional slopes where fire spread uphill. Moreover, for burned stands with medium-high LAI values, fire severity was higher in those dominated by small trees.

Discussion

The Yeste fire burned under high severirity conditions according to the RBR index (> 0.3) and near 60% of the fire area burned at fire severities high enough to kill most small *Pinus* trees (< 5 m). Our work shows that variations in fire severity (RBR) could be predicted with a relatively large capability. Burning conditions were the most relevant

set of explanatory variables in interaction with landscape features. We found that the fire front moving upslope and downwind had the fastest rate of spread and, under extreme weather conditions, produced the highest fire severities compared to flanking and backing portions of the fire. Prefire stand structure was also important for determining fire severity. Our results indicated that patches with small trees and high total biomass, including high understory vegetation, burned more severely than patches dominated by tall pine trees with low biomass in the understory; in accordance with a number of studies (Alexander et al. 2006). Thus, knowing stand structure and topography, if we are able to estimate the rate of spread and direction of the fire front based on the dominant winds, then fire severity could be anticipated. This indicates that it would be possible to implement fuel management treatments (e.g. reductions of surface fuels and small diameter trees in the understory) in specific areas (up or down slopes, fire front or flanks) to limit fire severity and, potentially, fire size (Safford et al. 2009). The availability of fire progression maps at different time steps, particularly for very large fires (Viedma et al. 2015) can be useful to better anticipate which factors control fire severity in a given area, and provide a basis for a more effective fire prevention planning.

References

Alexander JD, Seavy NE, Ralph CJ, Hogoboom B (2006) Vegetation and topographical correlates of fire severity from two fires in the Klamath-Siskiyou region of Oregon and California. *International Journal of Wildland Fire* **15**, 237-245

Axelsson P (2000) DEM generation from laser scanner data using adaptive TIN models. International archives of photogrammetry and remote sensing **33**, 110-117

De Santis A, Chuvieco E (2007) Burn severity estimation from remotely sensed data: Performance of simulation versus empirical models. *Remote Sensing of Environment* **108**, 422-435

Elith J, Leathwick JR, Hastie T (2008) A working guide to boosted regression trees. *Journal of Animal Ecology* **77**, 802-813

Forthofer JM (2007) Modeling wind in complex terrain for use in fire spread prediction. Ph.D. Thesis, Colorado State University Fort Collins.

Hijmans RJ, van Etten J (2012) Raster: Geographic analysis and modeling with raster data. R package version 2.0-12.

Isenburg M (2014) LAStools, "Efficient LiDAR Processing Software" (version 141017, academic), obtained from https://rapidlasso.com/LAStools/

Khosravipour A, Skidmore AK, Isenburg M (2016) Generating spike-free digital surface models using LiDAR raw point clouds: A new approach for forestry applications. *International Journal of Applied Earth Observation and Geoinformation* **52**, 104-114

Parisien MA, Parks SA, Miller C, Krawchuk MA, Heathcott M, Moritz MA (2011) Contributions of Ignitions, Fuels, and Weather to the Spatial Patterns of Burn Probability of a Boreal Landscape. *Ecosystems* **14**, 1141-1155

Parks, S, Dillon, G, Miller, C (2014) A new metric for quantifying burn severity: the Relativized Burn Ratio. *Remote Sensing* **6**, 1827-1844

R Core Team (2012) R: A language and environment for statistical computing. R Foundation for Statistical Computing, Vienna, Austria. http://www.R-project.org/

Ridgeway G (2007) GBM: Generalized Boosted Regression Models. R package version 1.6-3. http://www.i-pensieri.com/gregr/gbm.shtml.

Roussel JR, Auty D (2018) lidR: Airborne LiDAR Data Manipulation and Visualization for Forestry Applications. R package version 1.6.1. https://CRAN.R-project.org/package=lidR

Safford HD, Schmidt DA, Carlson CH (2009) Effects of fuel treatments on fire severity in an area of wildland-urban interface, Angora Fire, Lake Tahoe Basin, California. *Forest Ecology and Management* **258**, 773-787

Silva CA, Hudak AT, Vierling LA, Loudermilk EL, O'Brien JJ, Hiers JK, Jack SB, Gonzalez-Benecke C, Lee H, Falkowski MJ (2016) Imputation of individual Longleaf Pine (*Pinus palustris* Mill.) tree attributes from field and LiDAR data. *Canadian Journal of Remote Sensing* **42**, 554-573

Viedma O, Quesada J, Torres I, De Santis A, Moreno JM (2015) Fire severity in a large fire in a *Pinus pinaster* forest is highly predictable from burning conditions, stand structure, and topography. *Ecosystems* **18**, 237-250